


Effect of icariin on the H₂O₂-induced proliferation of mouse airway smooth muscle cells through miR-138-5p regulating SIRT1/AMPK/PGC-1 α axis

International Journal of
Immunopathology and Pharmacology
Volume 37: 1–15
© The Author(s) 2023
Article reuse guidelines:
sagepub.com/journals-permissions
DOI: 10.1177/03946320231151515
journals.sagepub.com/home/iji
SAGE

Yu-fang Huang, MD^{1,†}, Guo-chun Ou, MD^{1,†}, Shou-hong Ma, BD², Ming-wei Liu, MD³ 
and Wen Deng, BD⁴

Abstract

Icariin exerts antioxidative and anti-inflammatory effects and is used in the treatment of bronchial asthma. However, the specific modes of action are uncertain. In this study, we investigated whether icariin could modulate the silencing information regulator 2-related enzyme 1 (SIRT1)/adenosine monophosphate-activated protein kinase (AMPK)/peroxisome proliferator-activated receptor gamma co-activator 1 α (PGC-1 α) axis by regulating miR-138-5p during H₂O₂-induced proliferation of mouse airway smooth muscle cells (ASMCs). Primary BALB/c mouse ASMCs were cultured using the tissue block adherence method and were induced with hydrogen peroxide (H₂O₂; 200 μ mol/L) to establish a bronchial asthma ASMC proliferation model. With the aid of Western Blot and quantitative real-time polymerase chain reaction (qRT-PCR) in H₂O₂-induced ASMCs, the expression of miR-138-5p, SIRT1, AMPK, PGC-1 α , α -smooth muscle actin (α -SMA), transforming growth factor- β 1 (TGF- β 1), collagen I, and collagen III protein and mRNA were investigated. The proliferation rate and activities of superoxide dismutase I (SOD1), reduced glutathione (GSH), malonaldehyde (MDA), and reactive oxygen species (ROS) in ASMCs were determined. The results suggest Compared with the H₂O₂-induced group, icariin inhibited the miR-138-5p expression; enhanced SIRT1, p-AMPK, and PGC-1 α expression; attenuated MDA activity and ROS level; lowered TGF- β 1, collagen I, and collagen III expression levels; and decreased the proliferation of ASMCs induced by H₂O₂. The dual-luciferase reporter gene assay results showed that SIRT1 is a regulatory target of miR-138-5p. The results suggest that Icariin could improve the H₂O₂-induced proliferation of ASMCs. The mechanism may be related to the increase of activation of SIRT1/AMPK/PGC-1 α axis by suppressing the expression of miR-138-5p. Thus, SIRT1 is the regulatory target of miR-138-5p.

¹Department of Respiratory and Critical Care, Suining Central Hospital, Suining, China

²Medical Services Division, Sixth Affiliated Hospital of Kunming Medical University, Yuxi, China

³Department of Emergency, First Affiliated Hospital of Kunming Medical University, Kunming, China

⁴Department of Emergency, Suining Central Hospital, Suining, China

[†]These authors contributed equally to this work.

Corresponding authors:

Ming-wei Liu, Department of Emergency, First Affiliated Hospital of Kunming Medical University, 295 Xichang Road, Wu Hua District, Kunming 650051, China.

Email: lmw2004210@163.com

Wen Deng, Department of Emergency, Suining Central Hospital, No.127 Desheng West Road, Chuanshan District, Suining 69000, China.

Email: loveflower404@163.com



Creative Commons Non Commercial CC BY-NC: This article is distributed under the terms of the Creative Commons Attribution-NonCommercial 4.0 License (<https://creativecommons.org/licenses/by-nc/4.0/>) which permits non-commercial use, reproduction and distribution of the work without further permission provided the original work is attributed as specified on the SAGE and Open Access pages (<https://us.sagepub.com/en-us/nam/open-access-at-sage>).

Keywords

icariin, miR-138-5p, mouse airway smooth muscle cell, proliferation

Introduction

Asthma is an airway inflammatory illness that is characterized by airway inflammation, airway hyper-responsiveness, and airway remodeling, which is an important pathological change leading to irreversible airway obstruction and persistent deterioration of airway hyper-responsiveness.¹ In recent years, the incidence of bronchial asthma has increased significantly. Specific treatment is currently unavailable, and long-term repeated attacks and prolonged unhealing are prevalent, leading to airway remodeling, disease aggravation, and poor treatment effects, thus seriously threatening the health of patients with bronchial asthma. Therefore, the prevention and reduction of airway remodeling is useful for preventing and treating asthma.

An elevation in the level of free oxygen radicals and reactive oxygen species exacerbates airway injury and promotes airway smooth muscle cell (ASMCs) proliferation and airway remodeling.² MDA is one of the most important products of membrane lipid peroxidation. The degree of membrane lipid peroxidation can be understood through MDA, and SOD is responsible for converting superoxide to hydrogen peroxide. As second messengers, ROS play a role in controlling multiple cellular molecular pathways, such as the proinflammatory and pro-oxidative molecular pathways. Moreover, ROS enhances the multiplication of different cells and has crucial effects on the multiplication of ASMCs.³ In bronchial asthma, increased ROS and MDA levels or decreased SOD levels can disrupt the oxidative balance of the body and cause oxidative stress, leading to bronchial airway remodeling and promoting the occurrence and development of bronchial asthma.³ Therefore, controlling the production of ROS in airway tissues affected by bronchial asthma may inhibit airway remodeling induced by the disease and even its occurrence.

Epimedium is used to treat nephropathy,⁴ impotence,⁵ asthma,⁶ arthritis,⁷ and hypertension.⁸ Its main active ingredients are flavonoids, which contain icariin (ICA) and *Epimedium* polysaccharides. ICA is the primary active component of *Epimedium*. It has no obvious long-term toxicity and its clinical application is safe and reliable.⁹ It has immunomodulatory, anti-inflammatory, antioxidant, and other pharmacological properties that have an important impact on oxidative stress regulation in ASMCs and promote ASMC proliferation.¹⁰ However, its specific mechanism of action remains unclear.

Sirtuin 2-related enzyme 1 (SIRT1) can deacetylate proteins and plays a key role in oxidative stress.

Peroxisome proliferator-activated receptor-gamma co-activator 1 α (PGC-1 α) is an SIRT1 deacetylation substrate. The activation of SIRT1 can trigger PGC-1 α , thereby inhibiting oxidative stress damage.¹¹ Adenosine-activated protein kinase (AMPK) is an important enzyme that controls bioenergy metabolism and can improve mitochondrial dysfunction through PGC-1 α ; AMPK activity can be enhanced to promote cell survival.¹²

miRNAs play a significant role in the incidence and progression of bronchial asthma.¹³ MiR-138-5p gene expression can inhibit endotoxin-induced acute lung injury,¹⁴ whereas the overexpression of miR-138-5p can promote cardiomyocyte oxidative stress and cardiomyocyte apoptosis.¹⁵ Therefore, miR-138-5p may be implicated in H₂O₂-induced proliferation of ASMCs in mice. We identified SIRT1 as a possible regulatory target of miR-138-5p using TargetScan. Therefore, in this study, we hypothesized that *Epimedium* mediates the effect of the SIRT1/AMPK/PGC-1 α axis on H₂O₂-induced mouse ASMC proliferation by controlling miR-138-5p gene expression. Since the protective effect and mechanism of *Epimedium* on asthma mice with airway remodeling via regulated miR-138-5p has been scarcely reported, we conducted this study to explore the effect of *Epimedium* on asthma mice with airway remodeling and its functional mechanism as well as the potential role of miR-138-5p, hoping to provide new insights into the development of therapeutic drugs and the pursuit for gene therapy targets for asthma with airway remodeling.

Materials and methods

ASMC culture and grouping

Airway smooth muscle cells were grown in a culture medium known as 1640 medium containing 10% fetal bovine serum (Shanghai Cell Bank, Chinese Academy of Sciences, Shanghai, China). When the growth and fusion rates reached 70%, the ASMCs were cultured in a culture dish with a cell count of 1×10^4 /mL per well plate, cultured at a temperature of 37°C in a 5% CO₂ incubator, degraded with 0.25% trypsin, and cultured with 1:2 passage for 7 days. The cells were seeded at a density of 1×10^5 cell/mL in a 25 cm² culture flask. Upon reaching a cell fusion percentage of approximately 60%, the cells were grown synchronously for 24 h and then grouped. To determine the impact of H₂O₂ on ASMCs proliferation, based on previous research,¹⁶ different concentrations of H₂O₂ were added (20–300 μ mol/L), and the cells were cultured for

1 day. To determine the effect of ICA on ASMC proliferation triggered by H_2O_2 (200 $\mu\text{mol/L}$), we divided the ASMCs into normal, H_2O_2 -induced, H_2O_2 + ICA (50 $\mu\text{mol/L}$), H_2O_2 + ICA (150 $\mu\text{mol/L}$), and H_2O_2 + ICA (200 $\mu\text{mol/L}$) groups. Based on previous research,¹⁷ the H_2O_2 -induced and treatment groups were cultured with H_2O_2 (200 $\mu\text{mol/L}$) for 1 day, followed by the addition of ICA (50–200 $\mu\text{mol/L}$) for 24 h. The cell activities and levels of oxidative stress in the corresponding ASMCs were quantified, and real-time quantitative polymerase chain reaction (RT-qPCR) and western blotting were conducted.

Viability of the ASMCs were measured with a CCK-8 kit. The viability of ASMCs in the various treatment groups were determined using a CCK-8 kit. ASMCs were plated in 96-well plates and the confluence rate of cells reached 70–80%. The old culture solution was removed, and each group contained five pores. The experimental group was 100 μL per well, H_2O_2 (200 $\mu\text{mol/L}$) was added to the model group, and H_2O_2 (200 $\mu\text{mol/L}$) was added to the treatment group for 24 h. Based on previous research,¹⁸ ICA (50–200 $\mu\text{mol/L}$) was added to each well for 24 h, followed by 3 h of CCK-8 solution (10 L). A microplate reader at 450 nm was utilized for the purpose of determining the absorbance value (450 nm).

Transfection of ASMCs. An appropriate amount of logarithmic ASMCs was introduced into a 6-well plate. Based on previous research,¹⁹ after the ASMCs were allowed to adhere to 60%–70%, the miR-138-5p mimic, miR-138-5p inhibitor, miR-138-5p mimic control, and miR-138-5p inhibitor control were transfected into the ASMCs in accordance with Lipofectamine 2,000 protocols. The transfection concentration was 50 nM. A new culture medium was used after 6 h of transfection, and the culture was continued for 48 h. The cells were then collected for cell proliferation, RT-PCR, and western blotting.

MTT assay for proliferation rate of ASMCs. Airway smooth muscle cells were seeded in a 96-well plate and cell fusion of up to 70–80% was attained. The culture solution was discarded, and five wells were assigned to each group (100 μL /well in the experimental group). H_2O_2 (200 $\mu\text{mol/L}$) was introduced into the model group, and ICA (50–200 $\mu\text{mol/L}$) was added to the treatment group for 1 day. The fluid in each well of the 96-well plate was emptied, and 270 L of DMEM was introduced. Based on previous research,²⁰ 30 μL of 5 g/L MTT working solution was also introduced. The resulting solution was evenly mixed and incubated for 4 h at 37°C.

The medium in the wells was removed, and each well received 270 L of dimethyl sulfoxide. The solution was shaken for 10 min. A microplate reader was utilized for the purpose of detecting the OD value of every well at a wavelength of 490 nm. The cell proliferation and cell proliferation inhibition rates of the ASMCs in each well were calculated using the OD value of the normal group as the control group. Each measurement was repeated thrice, and the mean values were calculated. The following formula was used: cell proliferation rate (%) = OD value of each well/mean OD value of normal group \times 100%⁵; cell proliferation inhibition rate (%) = [1 – (OD value of experimental group OD value of blank hole)/(OD value of control group – OD value of blank hole)] \times 100%.⁵

EdU assay for detection of cell proliferation ability. Airway smooth muscle cells grown in log phase were seeded in 96-well cell culture plates, and the cell count in each well was $5 \times 10^3/\text{mL}$. Each group had five duplicate wells, and H_2O_2 (200 $\mu\text{mol/L}$) was added to the treatment and model groups. After 24 h of culture, ICA (10–50 $\mu\text{mol/L}$) was added for 24 h. Based on previous research,²¹ the cell culture medium was removed, followed by the addition of 50 $\mu\text{mol/L}$ EdU medium. Incubation of The cells were done for 2 h at a temperature of 37°C. The cells were fixed in 4% paraformaldehyde at room temperature for half an hour. Approximately 2 mg/mL glycine was incubated for 5 min at room temperature, followed by incubation for 10 min with 0.5% TritonX-100 at room temperature, PBS was rinsing with PBS. This was followed by the addition of 1 \times Apollo staining reaction solution and incubating the cells for half an hour at room temperature. The reaction solution was discarded, TritonX-100 was used to rinse the cells, and DAPI was used for the purpose of conducting nuclear staining. Fluorescence microscopy was used to observe cell luminescence. Red fluorescence was stained for EdU positivity and blue fluorescence was stained with DAPI.

Prediction of the miR-138-5p target gene. The target gene of miR-138-5p may be SIRT1 according to TargetScan (<http://www.targetscan.org/software>). Wild-type (Wt) SIRT1 and mutant (Mut) SIRT1 luciferase gene vectors were developed in accordance with the conventional methods. The two plasmids were mixed with miR-138-5p mimic control, miR-138-5p inhibitor control, miR-138-5p mimic, and miR-138-5p inhibitor co-transfected into ASMCs. They were designated as Wt + miR-138-5p mimics, Mut + miR-138-5pin, Wt + negative control, and Mut + negative control. After 48 h of culture in a 5% CO_2 and incubation at

Table 1. Primer sequence of RT-PCR analysis.

Gene	Primer
miR-138-5p	F-5'-GGAGCTGGTGTGGAATCA -3' R-5'-CAGTGCCTGTCGTGGAGT-3'
U6	F-5'-CTCGCTTCGGCAGCACA-3' R-5'-AACGCTTCACGAATTTGCGT-3'
SIRT1 mRNA	F-5'-CGCTGTGGCAGATTGTTATTAA-3' R-5'-TTGATCTGAAGTCAGGAATCCC-3'
AMPK mRNA	F-5'-CTCACCTCCTCCAAGTTATT -3' R-5'-TCAGATGGGCTTATACAGC-3'
PGC-1 α mRNA	F-5'-CTACAATGAATGCAGCCCTCTT -3' R-5'-TGCTCCATGAATTCTCGGTCTT-3'
SOD1 mRNA	F-5'-CAAAGATGGTGTGGCCGATG-3' R-5'-TTTCCACCTTTGCCCAAGTCA-3'
NF- κ B mRNA	F-5'-AGGAGAGGATGAAGGAGTTGTG-3' R-5'-CCAGAGTAGCCAGTTTTTGTG-3'
β -actin	F-5'-ATGGTGAAGGTCGGTGTG-3' R-5'-AACTTGCCGTGGGTAGAG-3'

37°C, Based on previous research,²² double luciferase activity was recorded with the aid of a double luciferase reporter gene kit. SIRT1 levels in ASMCs overexpressing miR-138-5p were detected by western blotting and RT-PCR.

Real-time quantitative PCR

Cell fusion of 70%–80% was achieved by planting ASMCs in 96-well plates. The culture medium was removed, and each group contained five pores. The cell density in the experimental group was 100 μ L per well. H₂O₂ (200 μ mol/L) was introduced into the model group, and H₂O₂ (200 μ mol/L) was introduced into the treatment group for 24 h before the addition of ICA (50–200 μ mol/L) for 24 h. Based on previous research,²³ a total RNA extraction kit was used to extract RNA from the ASMCs in each treatment group. A PrimeScript RT reagent kit was used to reverse-transcribe RNA into complementary DNA. SIRT1 mRNA and miR-138-5p expression were detected by RT-PCR. The reaction mixture was as follows: PCR primer, 2 μ L; SYBR Premix Ex TaqTM ii, 10 μ L; nuclease-free H₂O, 6 μ L; DNA template, 2 μ L; and total reaction volume, 20 μ L. Three parallel holes were created for each sample. The reaction system was then subjected to a polymerase chain reaction PCR. Based on previous research,²⁴ to detect the levels of miR-138-5p, a TaqMan miRNA assay kit was used to detect (Applied Biosystems, Foster City, CA, USA). Using the 2^{- $\Delta\Delta$ Ct} technique. The following were The reaction conditions: pre-denaturation for 30 s at 95°C, reaction for 5 s at 95°C, and annealing for 30 s at 60°C. Forty cycles were performed in total, and the primer series are depicted in Table 1. U6 was used as the miR-138-5p internal reference. To determine the expression level of the

SIRT1 gene, the cyclic threshold (Ct) of each gene was determined, and a comparison to the U6 gene was performed.

Western blotting was used in analyzing protein expression levels in cells

Airway smooth muscle cells were seeded in a 96-well plate and cell fusion of up to 70–80% was achieved. The old culture medium was removed, and each group contained five pores. The experimental group contained 100 μ L of each well. Then, H₂O₂ (200 μ mol/L) was added to the model group, and the treatment group was subjected to immersion for 24 h in H₂O₂ (200 μ mol/L) and then for 24 h in ICA (50–200 μ mol/L). Based on previous research,²⁵ approximately 150 μ L of RIPA cell lysis buffer was added and lysis was performed for 30 min on an ice bath for the extraction of total protein from each cell group. Centrifugation was performed for 15 min at 4°C, after which protein purity was determined using BCA protein quantitative kit. Approximately 50 μ g of protein extract was introduced into 10% SDS-PAGE for electrophoresis separation, followed by the addition of 5% skim milk for one and half hours. The respective primary antibodies, SIRT1, AMPK, β -actin, and PGC-1 α (1:1000) were added at 4°C, and the cultures were carried out throughout the night. The next day, the membrane was washed three times with TBST, and goat anti-rabbit IgG labeled with HRP was added (volume dilution ratio was 1:3,000). The reaction was performed for 1 h at room temperature. Then, using TBST, the membrane was washed three times for 10 min each time to develop the color. ECL chemiluminescence solution was then added. The gray value of the strip was evaluated using Image Lab, and β -actin was used as an internal reference.

Detection of intracellular ROS level

Airway smooth muscle cells were plated in 96-well plates and 70–80% confluency was achieved. The culture medium was removed, and each group contained five pores. The experimental group contained 100 μ L of each well. In addition, H₂O₂ (200 μ mol/L) was introduced into the model group, and the treatment group was immersed in H₂O₂ (200 μ mol/L) for 24 h and then in ICA (50–200 μ mol/L) for 24 h. Based on a previous study,²⁶ the culture medium was removed. 100 μ L of Diluted DCFH-DA (10 μ mol/L) was added to each well and the samples were incubated in a CO₂ incubator for 20 min at 37°C. The cells were gently rinsed three times with DMEM/F12, a serum-free medium, to remove DCFH-DA, which did not penetrate the cells. Cell extraction was then carefully performed. An emission wavelength (Em) of 525 nm and an excitation wavelength (Ex) of 488 nm were used to measure the fluorescence intensity before and after drug action through flow cytometry.

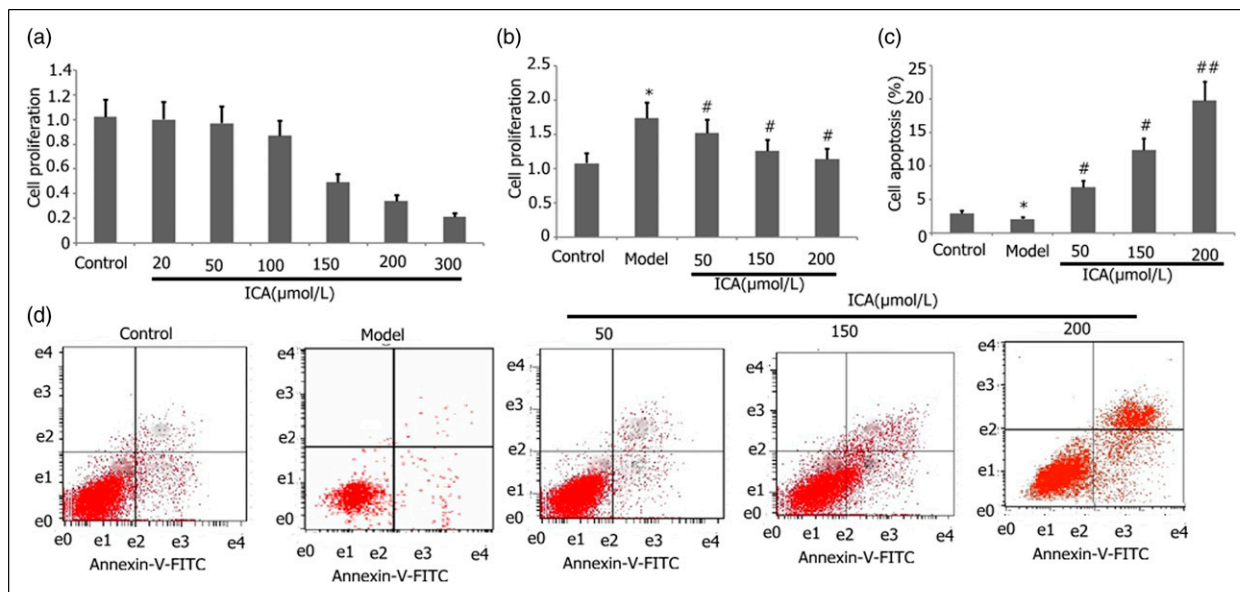


Figure 1. Effect of ICA on H_2O_2 -induced cell proliferation and apoptosis in H_2O_2 -induced ASMCs. ASMCs were incubated for 24 h in H_2O_2 (200 μ M) in the presence or absence of increasing concentrations of ICA (10, 20, and 50 μ M). (a and b): Cell proliferation in the ASMCs was measured using MTT. (c and d): Flow cytometry technique was employed in the quantification of cell apoptosis in ASMCs. Data obtained from three independent experiments were reported as mean \pm SD. * p < 0.05 versus the control group. # p < 0.05, ## p < 0.01 versus the H_2O_2 group. Control: control group; Model: model group (H_2O_2 group).

SOD, GSH activity, and MDA content detection

Based on previous research,²⁷ the cell homogenate of each group was placed on ice for lysis, and the supernatant was collected by centrifugation. SOD and GSH activity detection kits were used to detect SOD and GSH activity, respectively, and malonaldehyde levels were determined using a malonaldehyde content detection kit.

Colorimetric detection of caspase 3 and caspase 9 activities in cells

Airway smooth muscle cells were seeded in 96-well plates at 70–80% confluence. Before dosing the following day, the culture medium was discarded, and five replicate wells were set up in each group. The model group received H_2O_2 (200 μ mol/L) and the treatment group received H_2O_2 (200 μ mol/L). After culturing for 24 h, ICA (50–200 μ mol/L) was added and the cells were cultured for 24 h. The cells were isolated and lysed as previously described.²⁸ Following residue collection, activity was detected according to the instructions of the caspase 3 and caspase 9 kits, and the OD405 nm value was determined using a microplate reader.

Apoptosis detection

Airway smooth muscle cells were seeded in 96-well plates and grown to 70–80% confluence. Before dosing the next day, the old culture solution was discarded, and five wells were used in every group (100 μ L per well in the experimental group). H_2O_2 (200 μ mol/L) was introduced into the model group and ICA (50–200 μ mol/L) was added to the treatment group for 24 h. Based on previous research,²⁹ the samples were extracted, washed thrice in PBS, centrifuged for 5 min at 1200 r/min, suspended in 200 μ L of 1 \times binding buffer, mixed with 5 μ L of annexin V-EGFP, mixed with 5 μ L of propidium iodide, and reacted for 15 min in the dark at room temperature. Flow cytometry was used for the purpose of detecting Em of 530 nm and Ex of 488 nm. The FITC channel detected green fluorescence of annexin V-EGFP, whereas the PI channel detected red fluorescence of PI. Fluorescence compensatory regulation was performed using untreated normal cells to induce apoptosis as a control for removing spectral overlaps and setting the position of crosshairs.

Statistical analysis

GraphPad Prism 6 was used for all statistical analyses. The data obtained from the experiment are presented as the mean

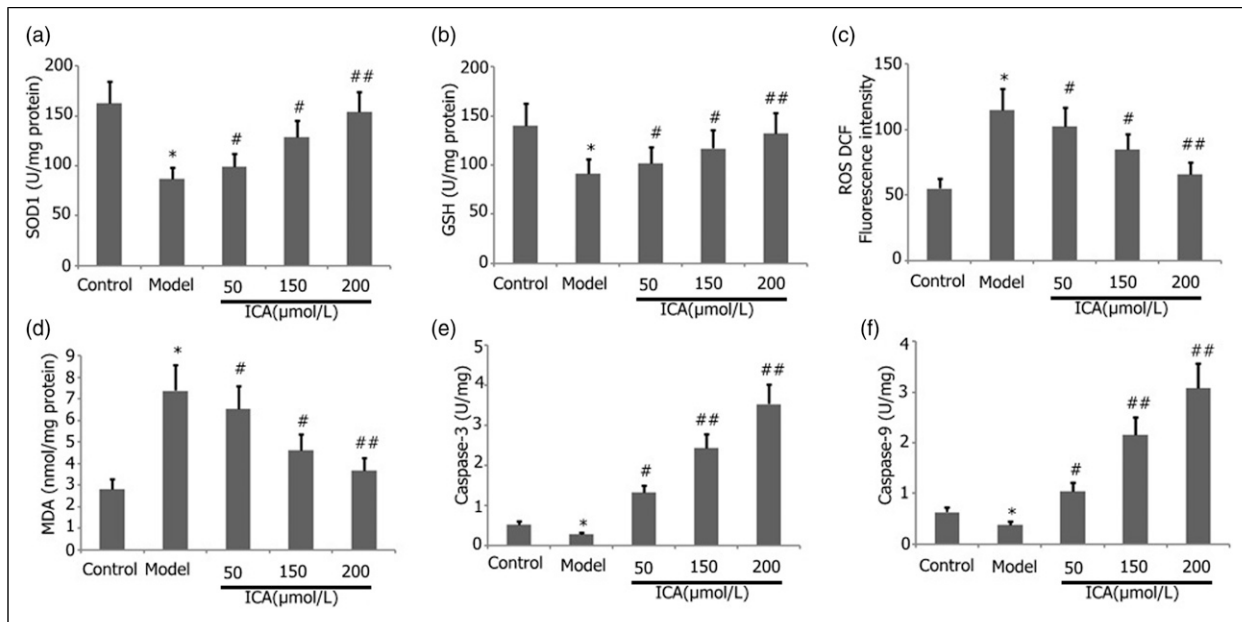


Figure 2. Effect of ICA on H_2O_2 -induced oxidative stress and activity of caspase 3 and 9 in ASMCs. ASMCs were incubated for 24 h in H_2O_2 (200 μM) in the presence or absence of increasing concentrations of ICA (10, 20, and 50 μM). (a and b): Cell proliferation was determined in the absence (A) and presence (B) of H_2O_2 -induced stress by MTT assay. (c and d): Apoptosis was determined by flow cytometric quantification of annexin V binding. (c). Quantification of apoptosis was determine by flow cytometric quantification of annexin V binding (d). Representative flow cytometry charts for cells treated without H_2O_2 (control), H_2O_2 alone (model), or H_2O_2 in the presence of ICA. The presentation of data obtained from three independent experiments was as mean \pm SD. * $p < 0.05$ versus the control group. # $p < 0.05$, ## $p < 0.01$ versus the only H_2O_2 group. Control: control group; Model: model group (H_2O_2 group).

\pm standard deviation. For conducting group comparisons, a one-way ANOVA was utilized, and for the comparison of pairwise significance between groups, the LSD method was utilized. Statistical significance was set at $p < 0.05$.

Results

ICA decreased H_2O_2 -induced cell proliferation and increased apoptosis in H_2O_2 -induced ASMCs

Inhibiting the proliferation of ASMCs and increasing their apoptosis can help reduce airway remodeling in patients with bronchial asthma. To investigate the effect of ICA on H_2O_2 -induced cellular proliferation and enhanced apoptosis in H_2O_2 -induced ASMCs, ASMCs were incubated for 24 h in H_2O_2 (200 $\mu mol/L$) and different concentrations of ICA (50, 150, and 200 $\mu mol/L$). Cell proliferation in ASMCs was measured using an MTT assay. Flow cytometry was used to detect apoptosis in the ASMCs. As depicted in Figure 1, ICA decreased H_2O_2 -induced cell proliferation and increased H_2O_2 -induced apoptosis (Figure 1(a)–(d)).

ICA decreased H_2O_2 -induced oxidative stress in ASMCs

Oxidative stress plays an important role in airway remodeling. To observe the effect of ICA on H_2O_2 -induced oxidative stress in ASMCs. ASMCs were incubated with H_2O_2 (200 $\mu mol/L$) and different concentrations of ICA (50, 150, and 200 $\mu mol/L$) for 24 h. The activities of ROS, SOD1, GSH1, and MDA were evaluated according to the manufacturer's guidelines. As shown in Figure 2, ICA decreased the H_2O_2 -induced activity of ROS and MDA (Figure 2(c) and (d)) and increased the activity of SOD1 and GSH1 in ASMCs (Figure 2(a) and (b)).

ICA decreased the activity of caspase 3 and caspase 9 in H_2O_2 -induced ASMCs

Caspase 3 and caspase 9 are important proapoptotic proteins. We observed the impact of ICA on the activity of both caspase 3 and caspase 9 in H_2O_2 -induced ASMCs. ASMCs were incubated for 24 h with H_2O_2 (200 $\mu mol/L$) and different

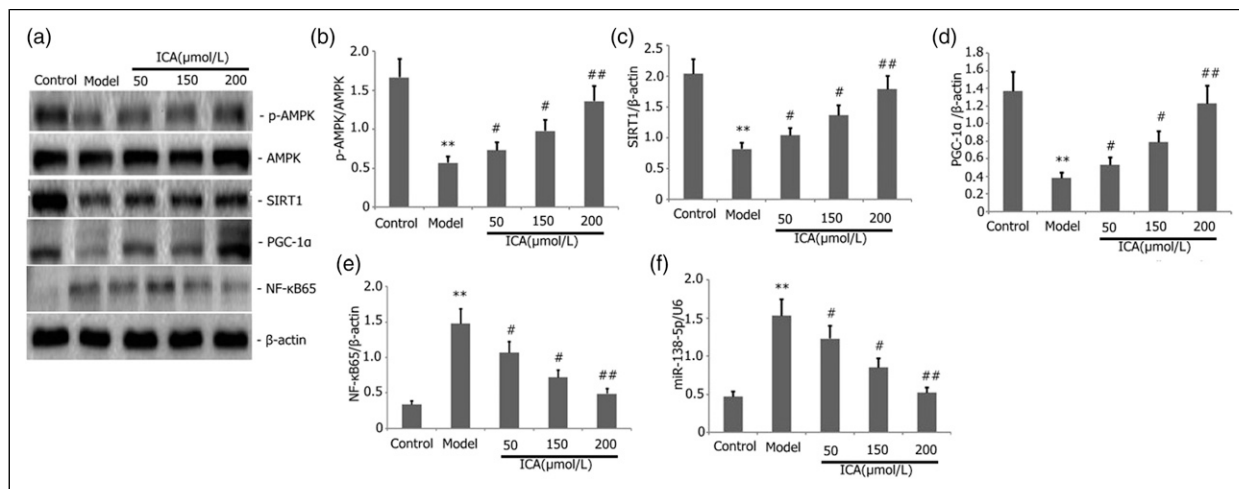


Figure 3. Effect of ICA on the activity of SIRT1/AMPK/PGC-1 α signaling pathway and miR-138-5p expression in H₂O₂-induced ASMCs. ASMCs were incubated for a duration of 24 h in H₂O₂ (200 μ mol/L) and various concentrations of ICA (10, 20, and 50 μ mol/L). (a–f): SIRT1, p-AMPK, NF- κ B65, and PGC-1 α protein expression levels were assayed using the Western blot technique. (g): The expression of miR-138-5p was assayed through RT-PCR. The data obtained from three independent experiments were reported as mean \pm SD. ** p < 0.01 versus the control group. # p < 0.05, ### p < 0.01 versus the H₂O₂ group. Control: control group; Model: model group (H₂O₂ group).

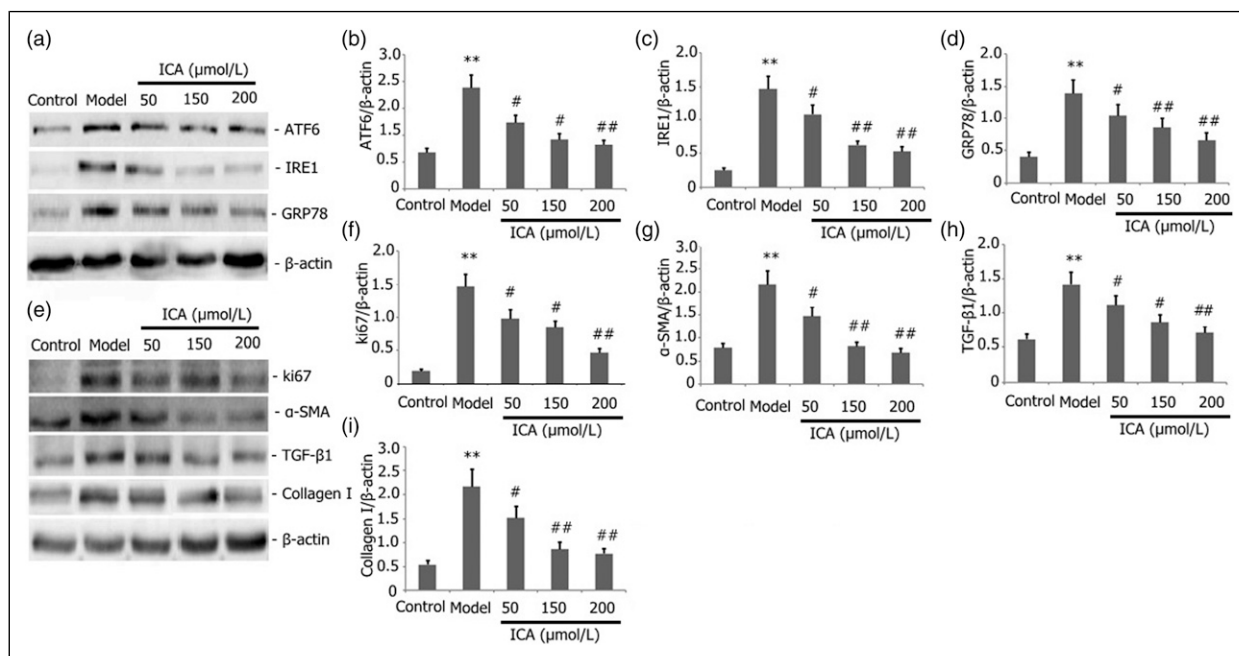


Figure 4. Effect of ICA on ATF6, IRE1, GRP78, ki67, α -SMA, TGF- β 1, and collagen I expression in H₂O₂-induced ASMCs. ASMCs were incubated in H₂O₂ (200 μ mol/L) and various concentrations of ICA (10, 20, and 50 μ mol/L) for 24 h. The expression of ATF6, IRE1, GRP78, ki67, α -SMA, TGF- β 1, and collagen I protein expression was measured through Western blotting. The presentation of data obtained from three independent experiments was as mean \pm SD. ** p < 0.01 versus the control group. # p < 0.05, ### p < 0.01 versus the H₂O₂ group. (a–d): Expression of ATF6, IRE1, and GRP78 protein in H₂O₂-induced ASMCs. (e–i): Expression of ki67, α -SMA, TGF- β 1, and collagen I protein expression in H₂O₂-induced ASMCs.

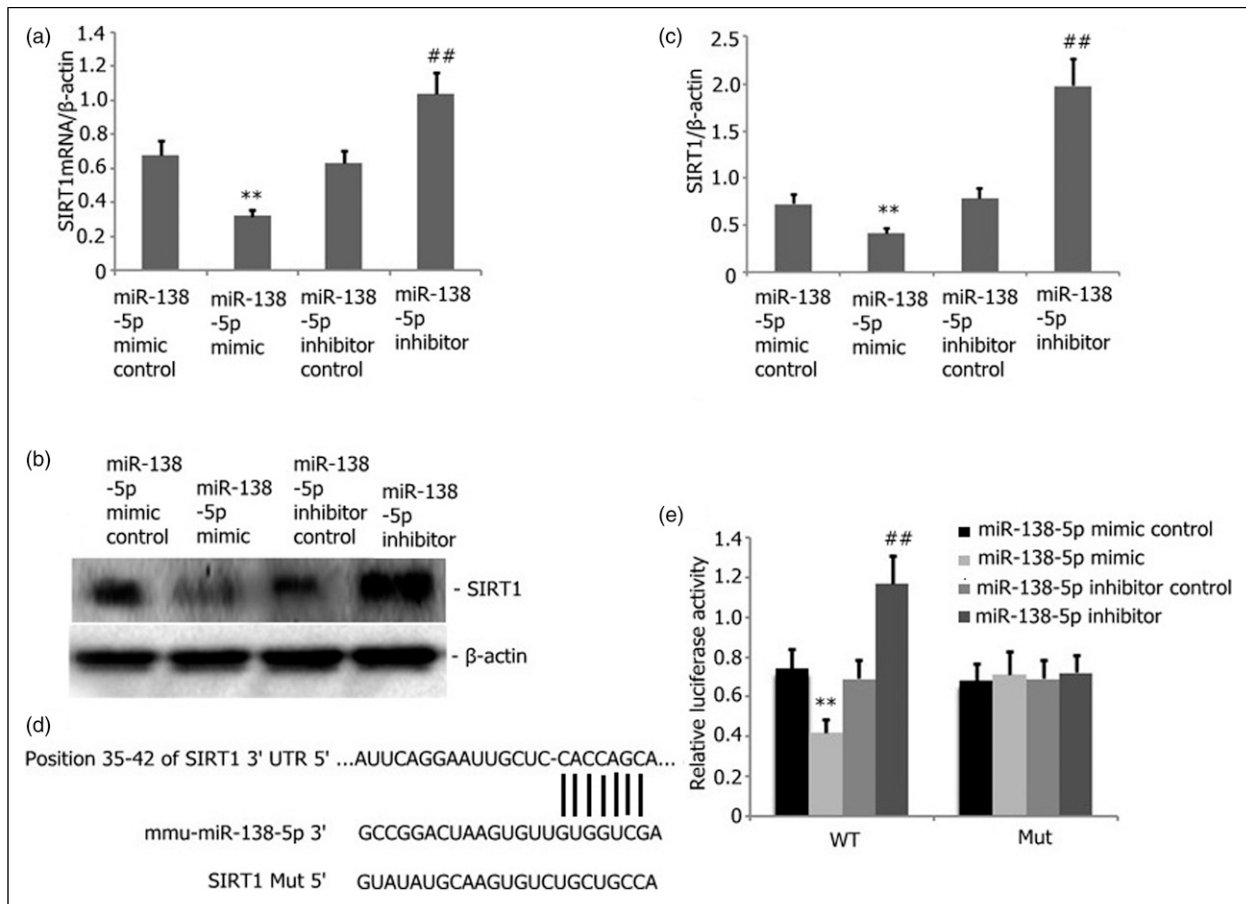


Figure 5. SIRT1 is a downstream target of miR-138-5p. (a–c): miR-138-3p was overexpressed in ASM cells and then RT-PCR and Western blotting used to determine SIRT1 mRNA and protein levels ($p < 0.01$). (d): miR-138-5p was bound to the 3'-UTR regions of SIRT1. Mutant SIRT1's binding was disrupted. E: Dual-luciferase reporter evaluation showed that the miR-138-5p mimic was bound to the 3'-UTR region of the wild-type SIRT1 rather than to the SIRT1 mutants ($p < 0.01$).

concentrations of ICA (50, 150, and 200 $\mu\text{mol/L}$). The activity of both caspase 3 and caspase 9 was assayed. As depicted in Figure 2, ICA increased the activity of both caspase 3 and caspase 9 in H_2O_2 -triggered ASMCs (Figure 2(e) and (f)).

ICA increased the activity of the SIRT1/AMPK/PGC-1 α signaling pathway and downregulated miR-138-3p expression in H_2O_2 -induced ASMCs

SIRT1/AMPK/PGC-1 α is an important pathway that regulates cellular oxidative stress and apoptosis. We investigated the influence of ICA on the function of the SIRT1/AMPK/PGC-1 α signaling pathway and downregulation of miR-138-3p expression in H_2O_2 -induced ASMCs. ASMCs were incubated with H_2O_2 (200 $\mu\text{mol/L}$) for 24 h at different concentrations of ICA (50, 150, and 200 $\mu\text{mol/L}$). The expression of miR-181a-5p, SIRT1, p-AMPK, NF- κB 65, and PGC-1 α mRNA was measured using RT-PCR, SIRT1, p-AMPK, and NF- κB 65, whereas PGC-1 α protein expression was evaluated

by western blotting. As depicted in Figure 3, ICA downregulated miR-138-3p expression (Figure 3(f)), increased SIRT1 p-AMPK and PGC-1 α protein expression (Figure 3(a)–(d)), and decreased NF- κB 65 protein expression in H_2O_2 -induced ASMCs (Figure 3(e)).

ICA decreased ATF6, IRE1, and GRP78 expression in H_2O_2 -induced ASMCs

ATF6, IRE1, and GRP78 are mainly involved in the regulation of cellular oxidative stress. We investigated the effect of ICA on ATF6, IRE1, and GRP78 expression in H_2O_2 -induced ASMCs. ASMCs were incubated for 24 h with H_2O_2 (200 $\mu\text{mol/L}$) and different concentrations of ICA (50, 150, and 200 $\mu\text{mol/L}$). ATF6, IRE1, and GRP78 protein expression levels were measured using western blotting. As shown in Figure 4(a)–(d), ICA decreased the expression of ATF6, IRE1, and GRP78 in H_2O_2 -induced ASMCs.

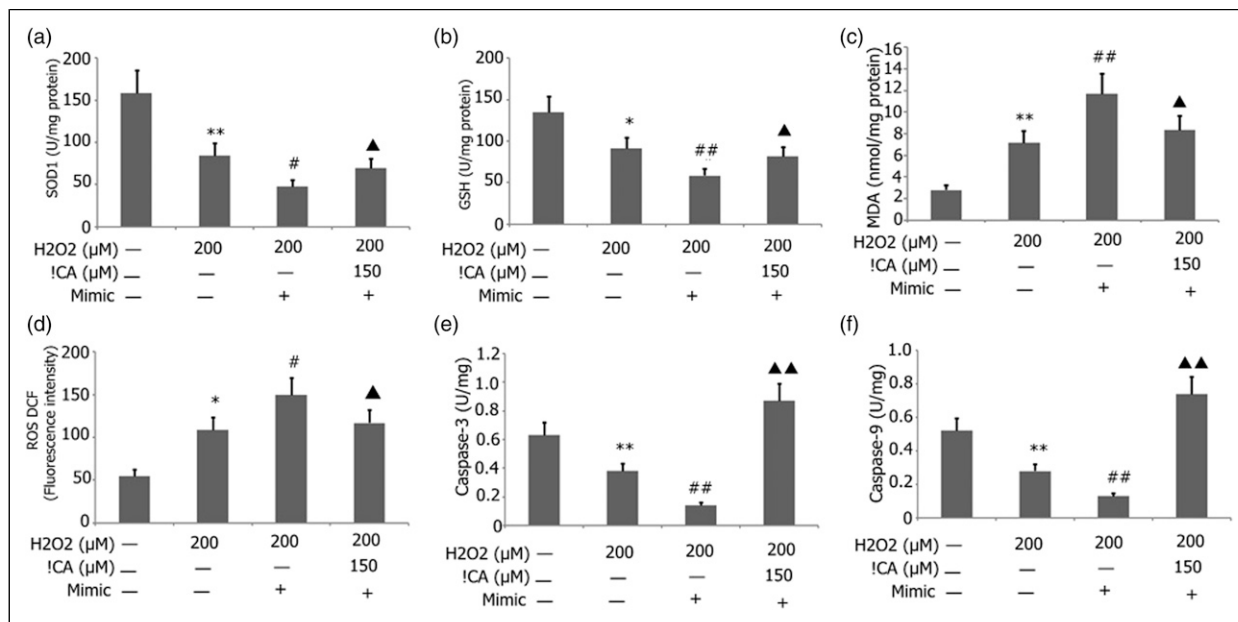


Figure 6. Effect of ICA and miR-138-3p mimic on H₂O₂-induced oxidative stress and the activities of caspase 3 and caspase 9 in ASMCs. The ASMCs were transfected for 24 h with a miR-138-3p mimic in the presence of H₂O₂ (200 μmol/L) and ICA (20 μmol/L). The activities of SOD1, ROS, MDA, caspase 3, and caspase 9 were assayed in accordance with the guidelines of the kit. The presentation of data obtained from 3 independent experiments was as mean ± SD. **p* < 0.05, ***p* < 0.01 versus the control group. #*p* < 0.05, ##*p* < 0.01 versus the H₂O₂ group. ▲*p* < 0.05, ▲▲*p* < 0.01 versus the mimic group. (a–d): The activities of SOD1, ROS, and MDA in H₂O₂-induced ASMCs. (e and f): The activities of caspase 3 and caspase 9 in H₂O₂-induced ASMCs. Mimic: miR-138-3p mimic.

ICA decreased *ki67*, α -SMA, TGF- β 1, and collagen I expression in H₂O₂-induced ASMCs

ki67 is an important marker for cell proliferation. α -SMA, TGF- β 1, and collagen I are involved in regulating cell proliferation and airway remodeling. In this study, we investigated the effect of ICA on *ki67*, α -SMA, TGF- β 1, and collagen I expression and found that ICA increased the activities of caspase 3 and caspase 9 in H₂O₂-induced ASMCs. ASMCs were incubated with H₂O₂ (200 μmol/L) and various concentrations of ICA (50, 150, and 200 μmol/L) for 24 h. The expression status of *ki67*, α -SMA, TGF- β 1, and collagen I proteins in H₂O₂-induced ASMCs was assessed by western blotting. As shown in Figure 4(e)–(i), ICA decreased the expression of *ki67*, α -SMA, TGF- β 1, and collagen I in H₂O₂-induced ASMCs.

SIRT1 is a regulatory target of miR-138-5p

We established that SIRT1 is a crucial regulator of H₂O₂-triggered ASMC proliferation. After overexpression of miR-138-5p, SIRT1 mRNA and protein levels were found to be significantly lower according to the results of statistical analysis (Figure 5(a)–(c)). TargetScan was used to predict the potential miR-138-5p targets to determine how miR-138-5p mediates ASMC proliferation through H₂O₂

induction (Figure 5(d)). We developed wild-type and mutant SIRT1 for a dual-luciferase reporter assay to verify the interplay between miR-138-5p and SIRT1. As expected, miR-138-5p bound to wild-type SIRT1 rather than to the mutants (Figure 5(e)).

Effect of ICA and miR-138-5p mimic on H₂O₂-induced oxidative stress and the activity of caspase 3 and caspase 9 in ASMCs

We analyzed the impact of ICA and the miR-138-5p mimic on H₂O₂-induced oxidative stress and the activity of both caspase 3 and caspase 9 in ASMCs. In the presence of H₂O₂ (200 mol/L) and ICA (150 mol/L), ASMCs were transfected with the miR-138-5p mimic for 24 h. The activities of MDA, ROS, GSH, SOD1, caspase 3, and caspase 9 were established in accordance with the manufacturer's guidelines. As depicted in Figure 6, the miR-138-5p mimic enhanced the H₂O₂-induced activities of ROS, MDA, caspase 3, and caspase 9 (Figure 6(c)–(f)), and attenuated the activities of SOD1 and GSH (Figure 6(a) and (b)). ICA decreased the miR-138-5p mimic-induced activities of ROS, MDA, and caspases 3 and 9 (Figure 6(c)–(f)) and increased the activities of SOD1 and GSH in H₂O₂-induced ASMCs (Figure 6(a) and (b)).

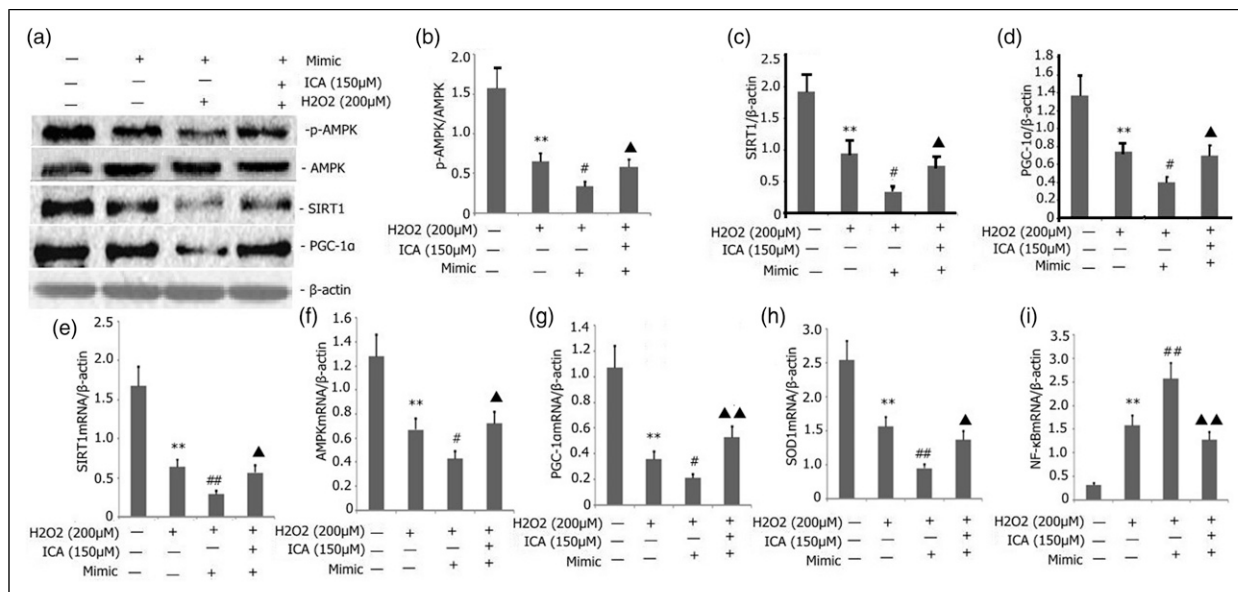


Figure 7. Effect of ICA and miR-138-3p mimic on the activity of the SIRT1/AMPK/PGC-1 α signaling pathway in H₂O₂-induced ASMCs. The ASMCs were transfected for 24 h with a miR-138-3p mimic in the presence of H₂O₂ (200 μ mol/L) and ICA (20 μ mol/L). (a–d): The Western blot technique assayed SIRT1, AMPK, and PGC-1 α protein expression. (e–i): SIRT1, AMPK, SOD1, NF- κ B, and PGC-1 α mRNA expression were assayed through RT-PCR. The data from 3 independent experiments were presented as mean \pm SD. ** p < 0.01 versus the control group. # p < 0.05, ## p < 0.01 versus the H₂O₂ group. ▲ p < 0.05, ▲▲ p < 0.01 versus the mimic group. Mimic: miR-138-3p mimic.

Effect of ICA and miR-138-5p mimic on the activity of the SIRT1/AMPK/PGC-1 α signaling pathway in H₂O₂-induced ASMCs

We analyzed the effect of ICA and miR-138-5p mimics on the function of the SIRT1/AMPK/PGC-1 α signaling pathway in H₂O₂-induced ASMCs. In the presence of H₂O₂ (200 mol/L) and ICA (150 mol/L), ASMCs were transfected with the miR-138-3p mimic for 24 h. The protein expression of SIRT1, AMPK, and PGC-1 α was evaluated by western blotting. The mRNA expression levels of SIRT1, AMPK, SOD1, NF- κ B, and PGC-1 α were evaluated by RT-PCR. As depicted in Figure 7, the miR-138-5p mimic lowered H₂O₂-induced SIRT1, AMPK, SOD1, and PGC-1 α mRNA (Figure 7(e)–(h)) and SIRT1, p-AMPK, and PGC-1 α protein expression levels (Figure 7(a)–(d)) and enhanced NF- κ B expression (Figure 7(i)), and ICA increased miR-138-3p mimic-induced SIRT1, AMPK, SOD1, and PGC-1 α mRNA (Figure 7(e)–(h)) and SIRT1, p-AMPK, SOD1, and PGC-1 α protein expression (Figure 7(a)–(d)) and

decreased NF- κ B expression (Figure 7(i)) in H₂O₂-induced ASMCs.

Effect of ICA and miR-138-5p mimic NF- κ B65, ki67, ATF6, IRE1, and GRP78 expression in H₂O₂-induced ASMCs

We analyzed the effects of ICA and miR-138-5p mimic on NF- κ B65, ki67, ATF6, IRE1, and GRP78 expression in H₂O₂-induced ASMCs. In the presence of H₂O₂ (200 mol/L) and ICA (150 mol/L), ASMCs were transfected for a duration of 24 h with the miR-138-3p mimic. The expression levels of ki67, ATF6, IRE1, NF- κ B65, and GRP78 in H₂O₂-induced ASMCs were assessed using western blotting. As depicted in Figure 8, miR-138-5p mimics increased H₂O₂-induced ki67, ATF6, IRE1, NF- κ B65, and GRP78 protein expression (Figure 8(a)–(g)), and ICA decreased miR-138-3p mimic-induced ki67, ATF6, IRE1, NF- κ B65, and GRP78 protein expression in H₂O₂-induced ASMCs (Figure 8(a)–(g)).

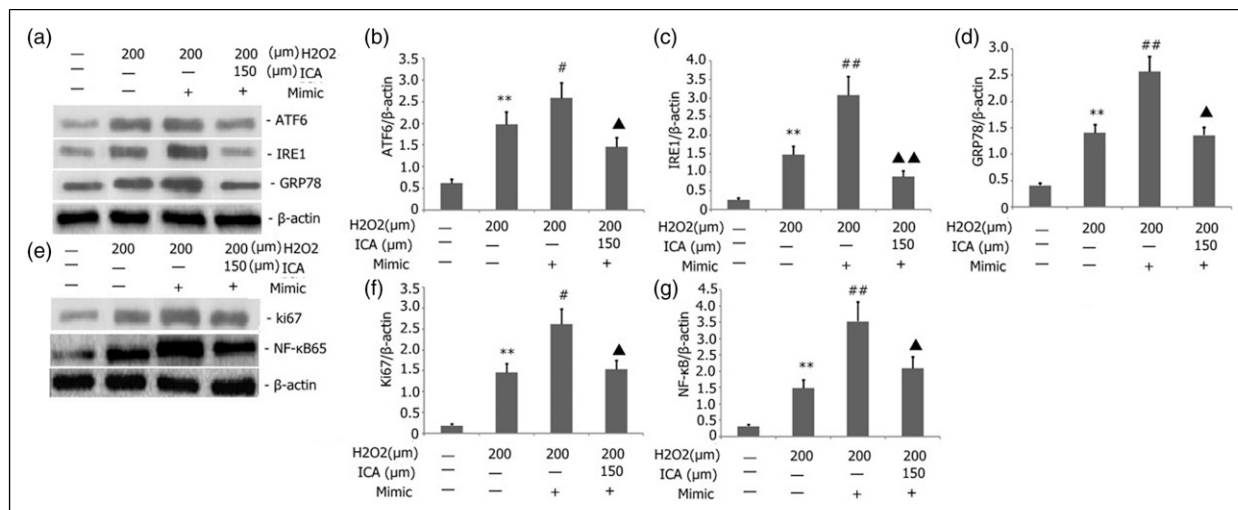


Figure 8. Effect of ICA and miR-138-3p mimic on H₂O₂-induced NF-κB65, ki67, ATF6, IRE1, and GRP78 in H₂O₂-induced ASMCs. The ASMCs were transfected for a duration of 24 h with a miR-138-3p mimic in the presence of H₂O₂ (200 μmol/L) and ICA (20 μmol/L). NF-κB65, ki67, ATF6, IRE1, and GRP78 protein expression were assayed by employing the Western blotting technique. The data obtained from 3 independent experiments were reported as mean ± SD. ***p* < 0.01 versus the control group. #*p* < 0.05, ##*p* < 0.01 versus the H₂O₂ group. ▲*p* < 0.05, ▲▲*p* < 0.01 versus the mimic group. (a–d): Expression of ATF6, IRE1, and GRP78 in H₂O₂-induced ASMCs. (e and f): Expression of NF-κB65 and ki67 in H₂O₂-induced ASMCs. Mimic: miR-138-3p mimic.

Effect of ICA and miR-138-5p mimic on α-SMA, TGF-β1, collagen I, and collagen III protein expression in H₂O₂-induced ASMCs

We analyzed the effect of ICA and the miR-138-5p mimic on TGF-β1, α-SMA, collagen I, and collagen III protein expression in H₂O₂-induced ASMCs. ASMCs were transfected with miR-138-5p mimics for 24 h in the presence of H₂O₂ (200 mol/L) and ICA (150 mol/L). Western blotting was used to quantify α-SMA, TGF-β1, collagen I, and collagen III protein expression. As shown in Figure 9, the miR-138-5p mimic increased H₂O₂-induced TGF-β1, α-SMA, collagen I, and collagen III protein expression (Figure 9(a)–(e)), whereas ICA decreased miR-138-3p mimic-induced α-SMA, TGF-β1, collagen I, and collagen III protein expression in H₂O₂-induced ASMCs (Figure 9(a)–(e)).

Effect of ICA and miR-138-5p mimic on H₂O₂-induced ASMC proliferation and apoptosis

We analyzed the impact of ICA and miR-138-5p mimics on H₂O₂-induced ASMC proliferation and apoptosis. ASMCs were transfected with miR-138-5p mimics for 24 h in the presence of H₂O₂ (200 mol/L) and ICA (20 mol/L). The EdU method was used to quantify ASMC proliferation. ASMC apoptosis was quantified by flow cytometry. As depicted in Figure 10, the miR-138-5p mimic increased H₂O₂-induced ASMC proliferation (Figure 10(a) and (b)) and reduced H₂O₂-induced ASMC

apoptosis (Figure 10(c) and (d)), whereas ICA decreased miR-138-3p mimic-induced ASMC proliferation (Figure 10(a) and (b)) and increased H₂O₂-induced ASMC (Figure 10(c) and (d)).

Discussion

Bronchial asthma is often accompanied by airway remodeling, which is closely related to poor prognosis and directly affects prognosis.^{30,31} When asthma occurs, ASMCs release a large number of free radicals after endogenous or exogenous damage, produce excessive oxidative substances such as ROS, induce the proliferation of ASMCs, promote airway remodeling in patients with asthma, and aggravate bronchial asthma.¹ Therefore, inhibiting oxidative stress may help to reduce airway remodeling, improve therapeutic effects, and improve the prognosis of patients with bronchial asthma. ICA treatment attenuated ROS production, H₂O₂-induced oxidative stress in ASMCs, and ASMC proliferation.

Studies have shown that activated AMPK (p-AMPK) acts on various downstream substrates, inhibits ATP consumption, initiates a pathway to generate ATP, maintains the body's energy metabolism balance, and increases the intracellular nicotinamide adenine dinucleotide content. SIRT1, which depends on nicotinamide adenine dinucleotide, is activated and exerts its corresponding biological effects.³² AMPK and SIRT1 regulate PGC-1α expression via phosphorylation and deacetylation, respectively. PGC-1α regulates the

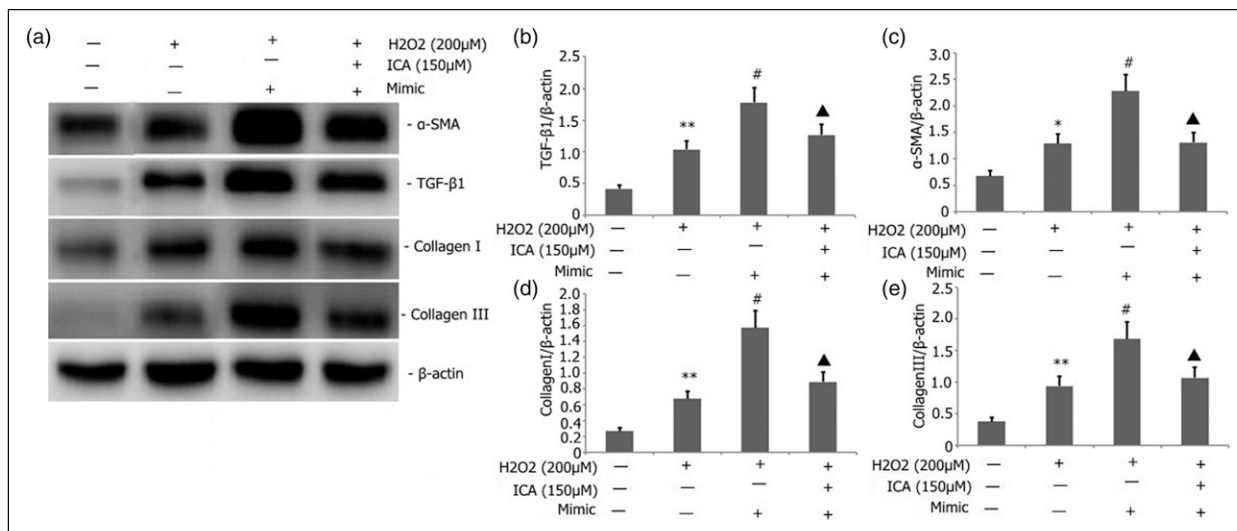


Figure 9. Effect of ICA and miR-138-3p mimic on H₂O₂-induced α -SMA, TGF- β 1, collagen I, and collagen III in H₂O₂-induced ASMCs. The ASMCs were transfected for a duration of 24 h with a miR-138-3p mimic in the presence of H₂O₂ (200 μ mol/L) and ICA (20 μ mol/L). (a–e): The expression levels of proteins of α -SMA, TGF- β 1, collagen I, and collagen III were assayed by employing the Western blot technique. The data obtained from 3 independent experiments were reported as mean \pm SD. * p < 0.05, ** p < 0.01 versus the control group. # p < 0.05 versus the H₂O₂ group. \blacktriangle p < 0.05 versus the mimic group. Mimic: miR-138-3p mimic.

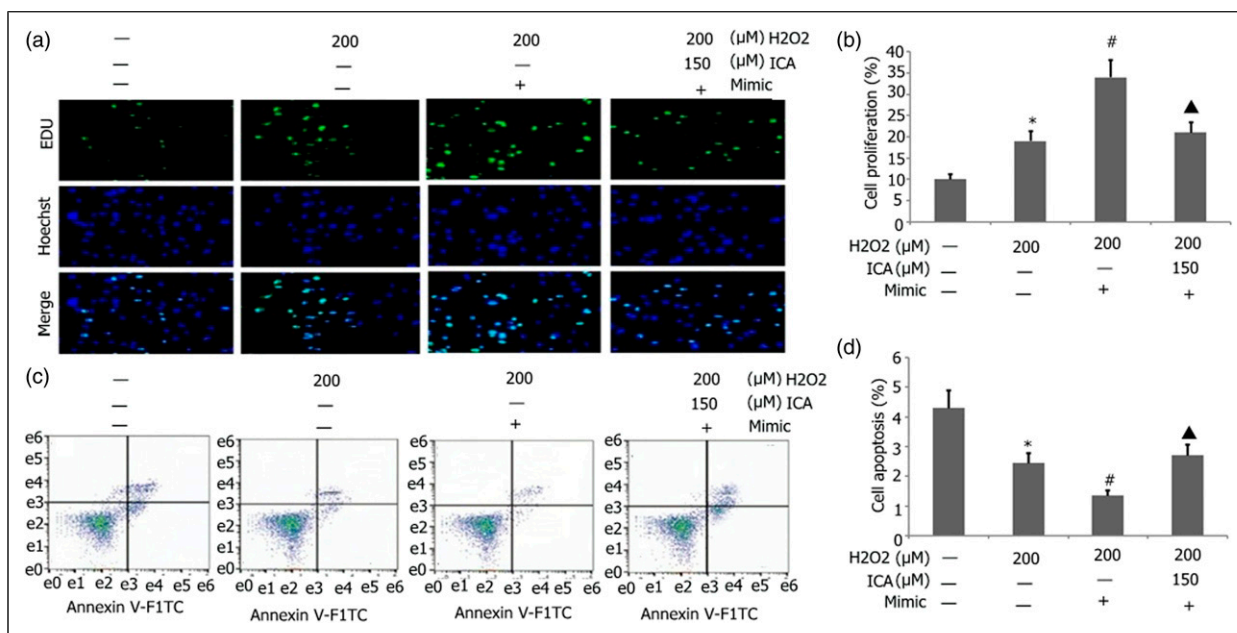


Figure 10. Effect of ICA and miR-138-5p mimic on H₂O₂-induced ASMC proliferation and apoptosis. ASMCs were transfected for a duration of 24 h with a miR-138-5p mimic in the presence of H₂O₂ (200 μ mol/L) and ICA (20 μ mol/L). (a and b): ASMC proliferation was assayed by applying the EdU method, (c and d): ASMC apoptosis was assayed by applying Flow cytometry. The data obtained from 3 independent experiments were reported as mean \pm SD. * p < 0.05 versus the control group. # p < 0.05 versus the H₂O₂ group. \blacktriangle p < 0.05 versus the mimic group. Mimic: miR-138-3p mimic.

activity of antioxidant enzymes and reduces MDA and ROS levels. It exerts an antioxidative stress effect, thereby protecting against myocardial ischemic injury.^{33,34} Moreover, SIRT1 can inhibit NF- κ B activity

by inducing AMPK and PGC-1 α activities.³⁵ It regulates the inflammatory and oxidative stress responses induced by various factors. In the present study, ICA treatment increased AMPK and SIRT1 expression, stimulated

PGC-1 α expression, increased SOD1 activity, decreased ROS activity, and reduced H₂O₂-induced oxidative stress. Furthermore, the activity of NF- κ B, inflammatory response of ASMCs induced by H₂O₂, and airway remodeling induced by H₂O₂ was further reduced. Serving as major ER stress sensors, ATF6 and IRE1 regulate ER protein folding by upregulating GRP78 and mediating XBP1 mRNA splicing, which is also an ER stress response factor.^{36–39} Therefore, ICA treatment may have decreased the expression levels of ATF6, IRE1, and GRP78 by increasing the activity of the AMPK/SIRT1/PGC-1 α pathway. The treatment decreased endoplasmic reticulum-induced oxidative stress translation in ASMCs, increased H₂O₂-induced ASMC apoptosis, and decreased H₂O₂-induced ASMC proliferation.

miRNAs have a pivotal impact on the onset and advancement of bronchial asthma,⁴⁰ controlling ASMCs' oxidative stress response, and growth and proliferation of ASMCs.⁴¹ MiR-133a expression is downregulated in asthmatic airway smooth muscle cells. It can cause excessive contraction by mediating calcium ions, aberrant proliferation, and death of ASMCs by upregulating RhoA expression.⁴² Increased expression of miR-10a inhibits ASMC hyperplasia. Conversely, suppression of the expression of miR-10a can remarkably reduce ASMC proliferation.⁴³ By targeting the regulation of zinc finger E-box-binding homeobox 2, miR-138-5p suppresses epithelial-mesenchymal transition, proliferation, and metastasis of lung adenocarcinoma cells.⁴⁴ By modulating cyclin-dependent kinase-8, miR-138-5p downregulation enhances non-small cell lung tumor advancement.⁴⁵ NF- κ B pathway activity, LPS-induced inflammation, and oxidative stress can be suppressed and LPS-induced acute lung injury can be relieved by inhibiting miR-138-5p expression.⁴⁶ In the present study, ICA treatment downregulated miR-138-5p expression, enhanced the function of the SIRT1/AMPK/PGC-1 α pathway, suppressed the activity of the NF- κ B pathway, and reduced H₂O₂-induced oxidative stress response and inflammatory reactions in ASMCs. This process also suppressed the formation of TGF- β 1, collagen I, and collagen III proteins and improved airway remodeling induced by H₂O₂. To clarify the reciprocal regulatory mechanism between miR-138-5p and SIRT1, a dual-luciferase reporter gene kit was used to detect dual-luciferase activity and to validate whether SIRT1 is the regulatory target of miR-138-5p. Their expression status in H₂O₂-induced ASMCs was negatively associated, implying that miR-138-5p modulates H₂O₂-induced ASMC activity and proliferation, as well as airway remodeling by regulating SIRT1 activity and expression.

ICA suppresses chondrocyte apoptosis and angiogenesis by controlling the TDP-43 signaling pathway.⁴⁷ It reduces inflammatory reactions caused by IL-1 β in

human nucleus pulposus cells.⁴⁸ It protects cardiomyocytes from ischemia or reperfusion damage by reducing mitochondrial oxidative stress caused by sirtuin 1.⁴⁹ It inhibits the IRE1 α -XBP1 signaling pathway to protect neurons from ER stress-induced apoptosis following oxygen and glucose deprivation or reperfusion injury.^{50,51} In the present study, ICA suppressed the function of NF- κ B by inhibiting the expression of miR-138-5 and activating the activities of AMPK and PGC-1 α . H₂O₂-induced oxidative stress and inflammation inhibited the activity and proliferation of H₂O₂-induced ASMCs and improved oxidative stress- and inflammation-induced airway remodeling.

Limitations of this study

This paper illustrated the protective mechanism of icariin on the H₂O₂-induced proliferation of mouse airway smooth muscle cells through miR-138-5p regulating SIRT1/AMPK/PGC-1 α axis. However, there are also some limitations in this study. First, the effect of miR-138-5p on SIRT1/AMPK/PGC-1 α in mouse airway smooth muscle cells may not be limited to oxidative stress-related proteins pathways. Inflammation, apoptosis, autophagy, pyroptosis, and other proteins and pathways might also be involved. Second, in addition to the SIRT1/AMPK/PGC-1 α pathway, many other pathways may be associated in the protective effects of icariin against H₂O₂-induced proliferation of mouse airway smooth muscle cells. The protective effect of icariin might involve inflammation, autophagy, pyroptosis, ferroptosis, and other processes. Further investigation must be conducted to determine the underlying mechanisms. The addition of an in vivo animal model would be valuable; however, no animal experiments were conducted in vivo in this study. In addition, the other target genes of miR-138-5p were not predicted in this study.

Conclusion

The present study demonstrates that ICA can improve H₂O₂-induced ASMC proliferation in mice. This mechanism could be linked to the reduction of oxidative stress by *Epimedium* in mouse ASMCs triggered by H₂O₂. This reduction was caused by the downregulated expression of miR-138-5p. This mechanism promotes SIRT1/AMPK/PGC-1 α axis activity. The regulatory target of SIRT1 was miR-138-5p. This study contributes to the understanding of the functional mechanism of ICA treatment for H₂O₂-induced ASMC proliferation in mice. The results promote the development of novel therapeutics and provide new gene targets for future studies. This work also provides an experimental cell basis for the ICA treatment of bronchial asthma with airway remodeling in clinical settings.

Declaration of conflicting interests

The author(s) declared no potential conflicts of interest with respect to the research, authorship, and/or publication of this article.

Funding

The author(s) received no financial support for the research, authorship, and/or publication of this article.

ORCID iD

Ming-wei Liu  <https://orcid.org/0000-0002-3728-2350>

References

- Boulet LP (2018) Airway remodeling in asthma: update on mechanisms and therapeutic approaches. *Current Opinion in Pulmonary Medicine* 24(1): 56–622.
- Cui J, Xu F, Tang Z, et al. (2019) Bu-Shen-Yi-Qi formula ameliorates airway remodeling in murine chronic asthma by modulating airway inflammation and oxidative stress in the lung. *Biomedicine and Pharmacotherapy* 112: 108694.
- Xian Z, Choi YH, Zheng M, et al. (2020) Imperatorin alleviates ROS-mediated airway remodeling by targeting the Nrf2/HO-1 signaling pathway. *Bioscience Biotechnology and Biochemistry* 84(5): 898–910.
- Xie C, Liu L, Wang Z, et al. (2018) Icariin improves sepsis-induced mortality and acute kidney injury. *Pharmacology* 102(3–4): 196–205.
- Xu Y, Xin H, Wu Y, et al. (2017) Effect of icariin in combination with daily sildenafil on penile atrophy and erectile dysfunction in a rat model of bilateral cavernous nerves injury. *Andrology* 5(3): 598–605.
- Hu L, Li L, Zhang H, et al. (2019) Inhibition of airway remodeling and inflammatory response by Icariin in asthma. *BMC Complementary and Alternative Medicine* 19(1): 316.
- Wei CC, Ping DQ, You FT, et al. (2016) Icariin prevents cartilage and bone degradation in experimental models of arthritis. *Mediators of Inflammation* 2016: 9529630.
- Xiang Y, Cai C, Wu Y, et al. (2020) Icariin attenuates monocrotaline-induced pulmonary arterial hypertension via the inhibition of TGF-beta1/smads pathway in rats. *Evidence-based Complementary and Alternative Medicine* 2020: 9238428.
- Ni G, Zhang X, Afedo SY, et al. (2020) Evaluation of the protective effects of icariin on nicotine-induced reproductive toxicity in male mouse –a pilot study. *Reproductive Biology and Endocrinology* 18(1): 65.
- Yang LH, Xiao B, Hou LX, et al. (2019) Bioactive molecule Icariin inhibited proliferation while enhanced apoptosis and autophagy of rat airway smooth muscle cells in vitro. *Cytotechnology* 71(6): 1109–1120.
- Liang D, Zhuo Y, Guo Z, et al. (2020) SIRT1/PGC-1 pathway activation triggers autophagy/mitophagy and attenuates oxidative damage in intestinal epithelial cells. *Biochimie* 170: 10–20.
- Tian L, Cao W, Yue R, et al. (2019) Pretreatment with Tiliarin improves mitochondrial energy metabolism and oxidative stress in rats with myocardial ischemia/reperfusion injury via AMPK/SIRT1/PGC-1 alpha signaling pathway. *Journal of Pharmacological Sciences* 139(4): 352–360.
- Weidner J, Bartel S, Kılıç A, et al. (2021) Spotlight on microRNAs in allergy and asthma. *Allergy* 76(6): 1661–1678.
- Wu Y, Jiang W, Lu Z, et al. (2020) miR-138-5p targets sirtuin1 to regulate acute lung injury by regulation of the NF-κB signaling pathway. *Canadian Journal of Physiology and Pharmacology* 98(8): 522–530.
- Chang Y, Xing L, Zhou W, et al. (2021) Up-regulating microRNA-138-5p enhances the protective role of dexmedetomidine on myocardial ischemia-reperfusion injury mice via down-regulating Ltb4r1. *Cell Cycle* 20(4): 445–458.
- Gülden M, Jess A, Kammann J, et al. (2010) Cytotoxic potency of H₂O₂ in cell cultures: impact of cell concentration and exposure time. *Free Radical Biology and Medicine* 49(8): 1298–1305.
- Song L, Chen X, Mi L, et al. (2020) Icariin-induced inhibition of SIRT6/NF-κB triggers redox mediated apoptosis and enhances anti-tumor immunity in triple-negative breast cancer. *Cancer Science* 111(11): 4242–4256.
- Lou J, Chu G, Zhou G, et al. (2010) Comparison between two kinds of cigarette smoke condensates (CSCs) of the cytogenotoxicity and protein expression in a human B-cell lymphoblastoid cell line using CCK-8 assay, comet assay and protein microarray. *Mutation Research* 697(1–2): 55–59.
- Wang LL, Dong JJ, An BZ, et al. (2020) Has-miR-17 increases the malignancy of gastric lymphoma by HSP60/TNFR2 pathway. *Journal of Biological Regulators and Homeostatic Agents* 34(4): 1317–1324.
- Wei CJ, Hua F, Chen YH, et al. (2021) Muscone alleviates myocardial ischemia-reperfusion injury via inhibition of oxidative stress and enhancement of SIRT3. *Journal of Biological Regulators and Homeostatic Agents* 35(1): 85–96.
- Gong Y, Yang J, Liu F, et al. (2018) Cyclin-dependent kinase 7 is a potential therapeutic target in papillary thyroid carcinoma. *Journal of Biological Regulators and Homeostatic Agents* 32(6): 1361–1368.
- Yasuno R, Mitani Y and Ohmiya Y (2018) Effects of N-Glycosylation deletions on cypridina luciferase activity. *Photochemistry and Photobiology* 94(2): 338–342.
- Li L, Dong Z, Shi P, et al. (2020) Bruceine D inhibits cell proliferation through downregulating LINC01667/MicroRNA-138-5p/Cyclin E1 axis in gastric cancer. *Frontiers in Pharmacology* 11: 584960.
- Tarazón E, de Unamuno Bustos B, Murria Estal R, et al. (2021) MiR-138-5p suppresses cell growth and migration in

- melanoma by targeting telomerase reverse transcriptase. *Genes (Basel)* 12(12): 1931.
25. Hirano S (2012) Western blot analysis. *Methods in Molecular Biology* 926: 87–97.
 26. Park E and Chung SW (2019) ROS-mediated autophagy increases intracellular iron levels and ferroptosis by ferritin and transferrin receptor regulation. *Cell Death & Disease* 10(11): 822.
 27. Kong D, Yan Y, He XY, et al. (2019) Effects of resveratrol on the mechanisms of antioxidants and estrogen in Alzheimer's disease. *BioMed Research International* 2019: 8983752.
 28. Zhang X and Malejka-Giganti D (2003) Effects of treatment of rats with indole-3-carbinol on apoptosis in the mammary gland and mammary adenocarcinomas. *Anticancer Research* 23(3B): 2473–2479.
 29. Darzynkiewicz Z, Bedner E and Smolewski P (2001) Flow cytometry in analysis of cell cycle and apoptosis. *Seminars in Hematology* 38(2): 179–193.
 30. Fehrenbach H, Wagner C and Wegmann M (2017) Airway remodeling in asthma: what really matters. *Cell and Tissue Research* 367(3): 551–569.
 31. Camoretti-Mercado B and Lockey RF (2021) Airway smooth muscle pathophysiology in asthma. *Journal of Allergy and Clinical Immunology* 147(6): 1983–1995.
 32. Cantó C, Gerhart-Hines Z, Feige JN, et al. (2009) AMPK regulates energy expenditure by modulating NAD⁺ metabolism and SIRT1 activity. *Nature* 458(7241): 1056–1060.
 33. Wang S, Wang C, Turdi S, et al. (2018) ALDH2 protects against high fat diet-induced obesity cardiomyopathy and defective autophagy: role of CaM kinase II, histone H3K9 methyltransferase SUV39H, Sirt1, and PGC-1 α deacetylation. *International Journal of Obesity (Lond)* 42(5): 1073–1087.
 34. Pereira AS, Gouveia AM, Tomada N, et al. (2020) Cumulative effect of cardiovascular risk factors on regulation of AMPK/SIRT1-PGC-1 α -SIRT3 pathway in the human erectile tissue. *Oxidative Medicine and Cellular Longevity* 2020: 1525949.
 35. Kauppinen A, Suuronen T, Ojala J, et al. (2013) Antagonistic crosstalk between NF- κ B and SIRT1 in the regulation of inflammation and metabolic disorders. *Cellular Signalling* 25(10): 1939–1948.
 36. Lebeau P, Byun JH, Yousof T, et al. (2018) Pharmacologic inhibition of S1P attenuates ATF6 expression, causes ER stress and contributes to apoptotic cell death. *Toxicology and Applied Pharmacology* 349: 1–7.
 37. Chopra S, Giovanelli P, Alvarado-Vazquez PA, et al. (2019) IRE1 α -XBP1 signaling in leukocytes controls prostaglandin biosynthesis and pain. *Science* 365(6450): eaau6499.
 38. Huang HW, Zeng X, Rhim T, et al. (2017) The requirement of IRE1 and XBP1 in resolving physiological stress during *Drosophila* development. *Journal of Cell Science* 130(18): 3040–3049.
 39. Chen CM, Wu CT, Chiang CK, et al. (2012) C/EBP homologous protein (CHOP) deficiency aggravates hippocampal cell apoptosis and impairs memory performance. *PLoS One* 7(7): e40801.
 40. van den Berge M and Tasena H (2019) Role of microRNAs and exosomes in asthma. *Current Opinion in Pulmonary Medicine* 25(1): 87–93.
 41. Yu H, Qi N and Zhou Q (2021) LncRNA H19 inhibits proliferation and migration of airway smooth muscle cells induced by PDGF-BB through miR-21/PTEN/Akt axis. *Journal of Asthma and Allergy* 14: 71–80.
 42. Chiba Y, Tanabe M, Goto K, et al. (2009) Down-regulation of miR-133a contributes to up-regulation of RhoA in bronchial smooth muscle cells. *American Journal of Respiratory and Critical Care Medicine* 180(8): 713–719.
 43. Hu R, Pan W, Fedulov AV, et al. (2014) MicroRNA-10a controls airway smooth muscle cell proliferation via direct targeting of the PI3 kinase pathway. *FASEB Journal* 28(5): 2347–2357.
 44. Zhu D, Gu L, Li Z, et al. (2019) MiR-138-5p suppresses lung adenocarcinoma cell epithelial-mesenchymal transition, proliferation and metastasis by targeting ZEB2. *Pathology Research and Practice* 215(5): 861–872.
 45. Xing S, Xu Q, Fan X, et al. (2019) Downregulation of miR-138-5p promotes non-small cell lung cancer progression by regulating CDK8. *Molecular Medicine Reports* 20(6): 5272–5278.
 46. Wu Y, Jiang W, Lu Z, et al. (2020) miR-138-5p targets sirtuin1 to regulate acute lung injury by regulation of the NF- κ B signaling pathway. *Canadian Journal of Physiology and Pharmacology* 98(8): 522–530.
 47. Huang H, Zhang ZF, Qin FW, et al. (2019) Icaritin inhibits chondrocyte apoptosis and angiogenesis by regulating the TDP-43 signaling pathway. *Molecular Genetics & Genomic Medicine* 7(4): e00586.
 48. Hua W, Zhang Y, Wu X, et al. (2018) Icaritin attenuates interleukin-1 β -induced inflammatory response in human nucleus pulposus cells. *Current Pharmaceutical Design* 23(39): 6071–6078.
 49. Wu B, Feng JY, Yu LM, et al. (2018) Icaritin protects cardiomyocytes against ischaemia/reperfusion injury by attenuating sirtuin 1-dependent mitochondrial oxidative damage. *British Journal of Pharmacology* 175(21): 4137–4153.
 50. Mo ZT, Liao YL, Zheng J, et al. (2020) Icaritin protects neurons from endoplasmic reticulum stress-induced apoptosis after OGD/R injury via suppressing IRE1 α -XBP1 signaling pathway. *Life Sciences* 255: 117847.
 51. He C, Wang Z and Shi J (2020) Pharmacological effects of icaritin. *Advances in Pharmacology* 87: 179–203.